Development and Validation of a 1D Oil-Injected Screw Compressor Model for Helium Compression

Scott Anthony[1*], Nusair Hasan[1], Venkatarao Ganni[1] and Abraham Engeda[2]

[1] Facility for Rare Isotope Beams (FRIB), Michigan State University, East Lansing, MI, USA
[2] Department of Mechanical Engineering, Michigan State University, East Lansing, MI, USA

[*]E-mail: anthonys@frib.msu.edu

Abstract. Oil-Injected twin screw compressors are widely used in cryogenic helium refrigeration systems as the prime mover. They provide all the thermodynamic availability for the cryogenic refrigeration system and account for more than one-half of the input power losses or two-thirds of total system availability losses. In general, cryogenic helium refrigeration systems use oil-injected screw compressors designed for air or traditional refrigerants, that are adopted for helium compression application. Both the low molecular weight and high specific heat of helium makes the compression process very challenging and requires a large quantity of oil for compression temperature control compared to other gas compression applications. These compression systems have relatively low system efficiencies and can benefit from understanding of the losses. A one-dimensional model is developed utilizing the energy and mass balance of the gas-oil mixture, including a well-established gas leakage correlation internal to the compressor. Simulations from the developed one-dimension model are compared to test data from a similar compressor. Primary parameters investigated in the present study include the pressure ratio, built in volume ratio, volumetric efficiency and isothermal efficiency. Such a predictive model can help to improve the helium compression process and thus the extremely energy intensive overall cryogenic system efficiency.

1. Background

This paper is a continuation of previously presented work [1]. For an overview of the working principes of an oil injected screw compressor, why oil-injected screw compressors are used for helium cryogenic applications, design challenges associated with helium compression, additional background information about the developed 1D model, and nomenclature not defined in this paper, reference [1]. For an efficient helium cryogenic plant, compressor system losses account for approximately one half of the total system input power [2-4] or two-thirds of overall system losses [5] (these losses are even greater for smaller systems, i.e. < 500 W or below at 4.5 K). Therefore, slight efficiency improvements to the compression process can significantly improve overall system efficiency, performance, and reliability. A simplified schematic of a compressor system skid is shown in Figure 1, the participation of the main components and the losses associated in the process with each component are labelled and shown. A Sankey diagram depicting the exergy flow and exergy losses associated with each component is also shown in Figure 1. The color of each exergy flow path corresponds a physical component, flow path, or loss of the same color. Note the relative size of each exergy flow path will change for different operating conditions, Figure 1 is shown as an example.

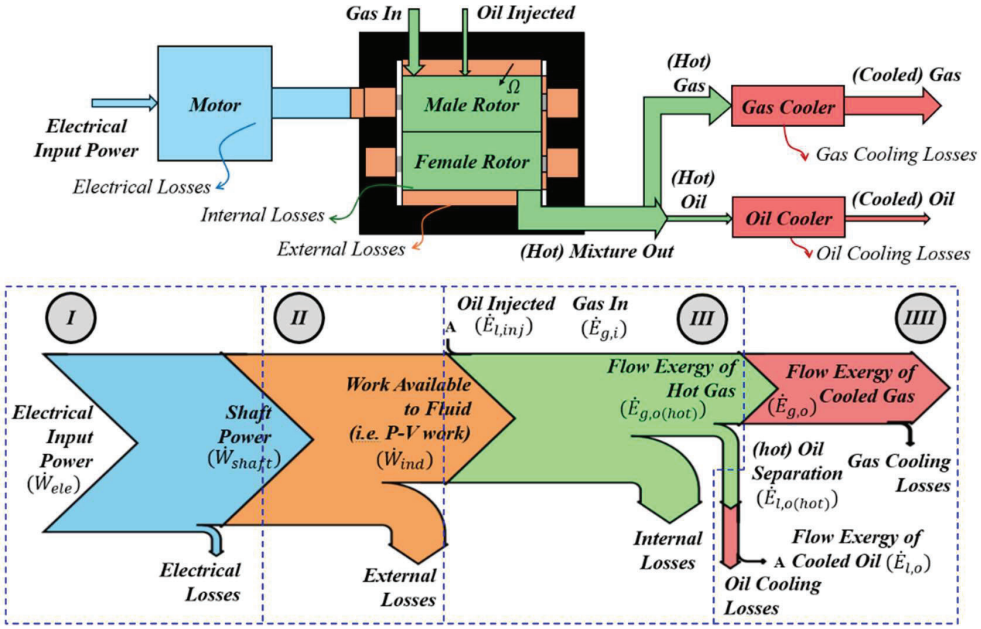

Figure 1. Schematic of Screw Compressor Losses: Components (top) and Exergy Flow (bottom)

The losses in Figure 1 include –

I: Drive losses due to motor and/or VFD inefficiencies.

II: External losses due to bearings, seals, and viscous power losses between rotors and casing.

III: Internal losses: due to leakage, oil-helium mixing loss, unmatched compression loss, and viscous heating loss.

IIII: Separation and cooling losses due to separating and cooling the hot oil and gas discharging from the compressor.

The purpose of this paper is to develop a 1D thermodynamic model of an oil-gas mixture through a screw compressor for helium compression. Then using the developed 1D model, evaluate volumetric efficiency, isothermal efficiency and how the magnitude of various losses are affected by pressure ratio (p_R) and built in volume ratio (BVR). BVR is the ratio of cavity volume when the suciton port closes to when the discharge port opens.

2. Model Development

2.1 Description of Model

The developed 1D model tracks an oil-gas mixture in one cavity (i.e. the control volume) as it progresses along the compressor rotors, from the low-pressure suction cavity to the high-pressure discharge cavity. Between the suction and discharge cavity, the oil-gas mixture is forced into sequentially smaller cavities, thus raising the pressure of the mixture. It is during this period that high pressure gas from a leading cavity can leak into the control volume and gas from the control volume can leak out to a low pressure trailing cavity. The gas internal leakage model has been incorporated following [6]. Also, during a period of this process, cooling oil is injected into the cavity. Oil temperature rises due to some of the gas heat of compression being transferred to the oil and viscous heating of oil due to the shear force along the lubricated clearances along the casing and rotors (Ω). Ω is defined later in this paper.

Assumptions for the developed 1D model are listed below, previously presented assumptions [1] also apply unless noted differently below:

- Only internal gas leakage is accounted for, no internal oil leakage [6]
- No leakage out of the control volume during the suction process [6]
- No leakage into the control volume during the discharge process [6]
- Leakage into the control volume only occurs when the leading pressure is higher [7]
- Leakage out of the control volume only occurs when the trailing pressure is lower [7]
- Leakage area profile as a function of angle of rotation of the screw is known (or derived from experimental data) as given in Eqn.(9)
- Electrical losses (I) are assumed to account for 4% of the electrical input power for this paper, shown in Eqn.(14).
- Viscous power losses between the rotors and casing is considered as an external loss ($\dot{P}_{external}$) and has been incorporated following Eqn.(11). External losses due to bearings and seals are assumed to be negligible
- Viscous heating, Ω, heats the oil directly [6] and goes into the gas. Ω is an internal loss.
- During under compression the flow from the discharge header into the control volume has the same temperature and oil-gas mass ratio as the control volume
- Oil-gas mixing loss, unmatched compression loss, and viscous heating loss are lumped and are given in Eqn.(23)

As previously noted, unless defined in this paper, nomenclature can be found here [1], where leakage terms contain a subscript *leak*. The overall gas phase and liquid (i.e. oil) phase energy and mass balance for the process are written below.

$$\frac{dm_g}{d\theta} = \frac{dm_{g,i}}{d\theta} - \frac{dm_{g,o}}{d\theta} + \frac{dm_{g,leak,i}}{d\theta} - \frac{dm_{g,leak,o}}{d\theta} \tag{1}$$

$$\frac{dm_l}{d\theta} = \frac{dm_{l,i}}{d\theta} - \frac{dm_{l,o}}{d\theta} + \frac{dm_{l,inj}}{d\theta} \tag{2}$$

$$\frac{dU_g}{d\theta} = \frac{dH_{g,i}}{d\theta} - \frac{dH_{g,o}}{d\theta} + \frac{dH_{g,leak,i}}{d\theta} - \frac{dH_{g,leak,o}}{d\theta} - \frac{dQ}{d\theta} + \frac{dW_g}{d\theta} \tag{3}$$

$$\frac{dU_l}{d\theta} = \frac{dH_{l,i}}{d\theta} - \frac{dH_{l,o}}{d\theta} + \frac{dH_{l,inj}}{d\theta} + \frac{dQ}{d\theta} + \frac{d\Omega}{d\theta} \tag{4}$$

Following the procedure outlined in Section 2.2 of [1], the change in gas temperature, oil temperature, and mixture pressure with respect to rotational angle were derived and are listed below. Since internal gas leakage was incorporated, the common factor (σ) includes a gas leakage term and is defined as $1+(m_{g,o}\gamma/m_g)+(m_{g,leak\,o}\gamma/m_g)$.

$$\frac{dT_g}{d\theta} = \frac{1}{\sigma}\left\{\frac{(\gamma T_{g,s} - T_g)}{m_g}\frac{dm_{g,i}}{d\theta} - \frac{(\gamma-1)T_g}{m_g}\frac{dm_{g,o}}{d\theta} + \frac{(\gamma T_{g,leak,i} - T_g)}{m_g}\frac{dm_{g,leak,i}}{d\theta} - \frac{(\gamma-1)T_g}{m_g}\frac{dm_{g,leak,o}}{d\theta} + \frac{m_{g,leak,i}\gamma}{m_g}\frac{dT_{g,leak,i}}{d\theta} - \frac{1}{\omega m_g c_{v,g}}(hA)(T_g - T_l) - \frac{(\gamma-1)T_g}{V_g}\frac{dV_g}{d\theta}\right\} \tag{5}$$

$$\frac{dT_l}{d\theta} = \frac{1}{(m_l + m_{l,o})}\left\{(T_{l,s} - T_l)\frac{dm_{l,i}}{d\theta} + (T_{l,inj} - T_l)\frac{dm_{l,inj}}{d\theta} + \frac{hA}{\omega c_{v,l}}(T_g - T_l) + \frac{1}{c_{vl}}\frac{d\Omega}{d\theta}\right\} \tag{6}$$

$$\frac{dp}{d\theta} = \frac{1}{\sigma}\left\{\frac{(\gamma T_{g,s} - T_g + \sigma T_g)R}{V_g}\frac{dm_{g,i}}{d\theta} - \frac{(\gamma - 1 + \sigma)p}{m_g}\frac{dm_{g,o}}{d\theta} + \frac{(\gamma T_{g,leak,i} - T_g + \sigma T_g)R}{V_g}\frac{dm_{g,leak,i}}{d\theta} - \frac{(\gamma - 1 + \sigma)p}{m_g}\frac{dm_{g,leak,o}}{d\theta} + \frac{m_{g,leak,i}\gamma R}{V_g}\frac{dT_{g,leak,i}}{d\theta} - \frac{(\gamma-1)}{\omega V_g}(hA)(T_g - T_l) - \frac{p(\gamma - 1 + \sigma)}{V_g}\frac{dV_g}{d\theta}\right\} \tag{7}$$

2.2 Nominal Versus Actual Leakage Flow Area

Nominal leakage path flow areas with respect to angle of rotation is a required input to the 1D model and is known if the compressor geometry is known. However, during operation, the

effective leakage flow area may be reduced due to the injected oil. Additionally, nominal leakage path area for a specific compressor is subjected to the actual tolerances in machining and assembly of all parts. To account for this a leakage flow coefficient can be multiplied to reduce the nominal leakage path area, resulting in an effective flow area [6], however not much is known about this factor. To determine the effective flow area, experimental data from the compressor simulated later in this paper was used [5]. Assuming choked flow (for p_R >2) through an orifice, continuously from the discharge header pressure to the suction header pressure, the effective leakage flow area was calculated for different built in volume ratios and pressure ratios. Gas leakage flow rate was calculated using the experimentally measured volumetric efficiency [5] and known ideal displacement capacity of the compressor. The effective leakage flow area appears to be independent of compressor BVR and a curve fit was used to determine the effective leakage flow area at different pressure ratios. The equation of this curve fit is shown in Eqn. (8) and is for this specific compressor and operating conditions. Equation (8) is the effective area for a continuous leakage rate for the entire compression cycle ($d\theta_{cycle}$). However, leakage only occurs when a leakage port is open ($d\theta_{leak}$) for a given cavity. Equation (9) is the effective leakage area when leakage ports are open and is used in the developed 1D model. This method of determining the effective leakage area can also be used if nominal compressor leakage path area is unknown, and as a way to verify provided nominal leak path area magnitude.

$$A_{eff\ leak,cont} = 115.5 p_R^{-0.552} \tag{8}$$

$$A_{eff\ leak,port} = A_{eff,cont} \frac{d\theta_{cycle}}{d\theta_{leak}} \tag{9}$$

2.3 Viscous Power Losses and Viscous Heating

Viscous power losses between the rotors and casing arise when an oil film fills the nominal clearance between the rotor tip and housing (c). Depending on the p_R, the nominal clearance area ($A_{nominal}$) is filled by both gas (Eqn.(8)) and oil ($A_{oil\ film}$), Eqn. (10). Following [8], the torque required to overcome the shear stress of the oil film for a lubricated bearing is modified for the rotor geometry and multiplied by the fraction of the nominal clearance filled by the oil, Eqn.(11). Inputs to this equation include oil dynamic viscosity (μ), fraction that the male and female rotor overlap (f), rotor diameter (d_{rotor}) and rotor length (l_{rotor}). Viscous heating due to viscous power loss into the control volume is given in Eqn.(12), heat is added to one cavity during the compression process when oil is present ($\theta_B - \theta_{A^*}$), using rotation speed (N) and number of male cavities (z_1).

$$A_{oil\ film} = A_{nominal} - A_{eff\ leak,cont} \tag{10}$$

$$\dot{P}_{external} = \frac{A_{oil\ film}}{A_{nominal}} \mu \frac{2\pi^3 (1-f) N^2 d_{rotor}^3 l_{rotor}}{c} \tag{11}$$

$$\Omega = \frac{\dot{P}_{external}}{z_1 N (\theta_B - \theta_{A^*})} \tag{12}$$

2.4 1D Model Inputs and Outputs

A Runge-Kuta 4th order method was written to simultaneously solve equations (5)-(7). Required model inputs, outputs and parameters used to run simulations later in this paper include:

- Fluid – Helium (γ=1.67 and R = 2.077 J/g-K)
- Compressor: Howden WLViH321193 (i.e. cavity volume, suction port areas, discharge port areas, oil injection port area, and nominal leakage path areas with respect to angle of rotation of the screw are known)
- Effective Leakage area (calculated from Eqn.(*9*))
- Initial gas temperature: 290 K

- Gas discharge temperature: 365 K (maintained by varying oiling injection mass flow rate)
- Gas suction pressure: 1.05 bara
- Oil injection pressure: discharge pressure
- Oil injection temperature: 313 K
- Axial and Radial discharge ports opens at V_R = 2.2, 3.0, or 3.4
- Rotor rotational speed 3566 rpm

A constant heat transfer coefficient (h) was used with a value of 22.8 kW/m^2-K and mean oil droplet diameter of 0.05 mm. This was determined by assuming a constant Nusselt number between the helium compression case in this paper and the R22 compression case in [1], then multiplying the R22 heat transfer coefficient of 1.7 kW/m^2-K by the thermal conductivity ratio of helium to R22 (i.e. 13.34 at NBP). Oil with a nominal density of 817 kg/m^3 and specific heat of 2.2 J/g-K was considered of the simulation. Ω is calculated flowing Eqn.(12). A constant discharge flow coefficient of 0.6 was used. Figure 3 presents outputs from the developed 1D model: gas temperature, oil temperature, mixture pressure, oil mass and gas mass with respect to rotation angle. P-V work (indicated work, W_{ind}) is an output of the 1D model because the compressor cavity volume (V_{cavity}) is known and is used to calculate indicated power ($\dot{W}_{ind}$) [9], shown Eqn.(13).

$$\dot{W}_{ind} = \frac{W_{ind} z_1 N}{60}, where \qquad W_{ind} = \int_{\theta_0}^{\theta_f} p dV_{cavity} \tag{13}$$

2.5 Compressor Skid Characterization

The present model assumes electrical losses ($\dot{P}_{ele}$) account for 4% of the electrical input power, from operational observations, and is given in Eqn.(14). Total electrical input power to the compressor is equal to the sum of $\dot{P}_{ele}$, $\dot{P}_{external}$, and $\dot{W}_{ind}$ and can be simplified by applying the previously described assumption, shown in Eqn.(15).

$$\dot{P}_{ele} = 0.04\dot{W}_{ele} \tag{14}$$

$$\dot{W}_{ele} = \dot{P}_{ele} + \dot{P}_{external} + \dot{W}_{ind} = 1.04(\dot{P}_{external} + \dot{W}_{ind}) \tag{15}$$

Now, the two main screw compressor performance parameters can be calculated from the 1D model. Skid isothermal efficiency ($\eta_{iso,skid}$) is the ratio of the isothermal power to the electrical input power and volumetric efficiency (η_v) is the ratio of the measured actual mass flow rate ($\dot{m}_{actual}$) to the theoretical maximum mass flow rate ($\dot{m}_{theoretica}$) through a screw compressor, defined in Eqn.(16) and Eqn.(17), respectively.

$$\eta_{iso,skid} = \frac{\dot{W}_{iso}}{\dot{W}_{ele}} \tag{16}$$

$$\eta_v = \frac{\dot{m}_{actual}}{\dot{m}_{theoretical}} \tag{17}$$

3. Breakdown of Losses

As shown in Figure 1, separation and cooling losses ($\dot{P}_{s\&c}$) is this difference in flow exergy of the gas and oil into and out of their respective coolers, defined in Eqn.(18). Where flow exergy of an ideal gas is defined in Eqn.(19) and for an incompressible fluid in Eqn.(20). Reference exergy (ε_0) is taken at the compressor gas suction temperature (T_0) and pressure (p_0). This loss is calculated using model inputs and outputs.

$$\dot{P}_{s\&c} = \dot{E}_{g,o(hot)} + \dot{E}_{l,o(hot)} - \dot{E}_{g,o} - \dot{E}_{l,o} \tag{18}$$

$$\dot{E}_g = \dot{m}_g\left[\left(h_g - T_0 s_g\right) - \varepsilon_0\right] \tag{19}$$

$$\dot{E}_l = \dot{m}_l \left[c_{p,l}(T_l - T_0) - T_0 c_{p,l} \, ln\left(\frac{T_l}{T_0}\right)\right] \quad (20)$$

Also shown in Figure 1, the total internal losses ($\dot{P}_{internal(total)}$), can be written as Eqn.(21) where useful exergy discharging from the compressor ($\dot{E}_{g,o}$) is calculated from the 1D model.

$$\dot{P}_{internal(total)} = \dot{W}_{ind} - \dot{P}_{s\&c} - \dot{E}_{g,o} \quad (21)$$

Total internal losses can be separated into two components: internal leakage losses ($\dot{P}_{internal(leak)}$) and miscellaneous internal losses ($\dot{P}_{internal(misc)}$). Internal leakage losses arise from recirculating gas that leaks along internal compressor leakage paths. The indicated power is proportionally scaled using the leakage mass to estimate the additional power required by compression of this mass, Eqn.(22). The remaining internal losses, $\dot{P}_{internal(misc)}$, are a lumped term accounting for additional work due to unmatched compression, non-ideal oil-gas mixing, and accelerating injected oil along the rotors, Eqn.(23). These miscellaneous losses will be separated and independently calculated in the future.

$$\dot{P}_{Internal(leak)} = (1 - \eta_v)\dot{W}_{ind} \quad (22)$$

$$\dot{P}_{internal(misc)} = \dot{P}_{internal(total)} - \dot{P}_{internal(leak)} \quad (23)$$

The previously defined losses are written as a ratio of electrical input power in Eqn.'s(24)–(27): electrical losses (Ψ_{ele}), external losses ($\Psi_{external}$), total internal losses ($\Psi_{internal(total)}$), internal leakage losses ($\Psi_{internal(leak)}$), miscellaneous internal losses ($\Psi_{internal(misc)}$), and separation and cooling losses ($\Psi_{c\&s}$).

$$\Psi_{ele} = \frac{\dot{P}_{ele}}{\dot{W}_{ele}} = 0.04 \quad (24)$$

$$\Psi_{external} = \frac{\dot{P}_{external}}{\dot{W}_{ele}} \quad (25)$$

$$\Psi_{internal(total)} = \frac{\dot{P}_{internal(total)}}{\dot{W}_{ele}} = \left[\left(\Psi_{internal(leak)} = \frac{\dot{P}_{internal(leak)}}{\dot{W}_{ele}}\right) + \left(\Psi_{internal(misc)} = \frac{\dot{P}_{internal(misc)}}{\dot{W}_{ele}}\right)\right] \quad (26)$$

$$\Psi_{c\&s} = \frac{\dot{P}_{s\&c}}{\dot{W}_{ele}} \quad (27)$$

4. Results and Discussion

Simulations were performed using the compressor and input parameters from Section 2.4. Variation in $\Psi_{internal(total)}$, $\Psi_{internal(leak)}$, and $\Psi_{internal(misc)}$ with respect to BVR and pressure ratio is presented in Figure 2. $\Psi_{internal(leak)}$ remained relatively flat over the range of BVRs and pressure

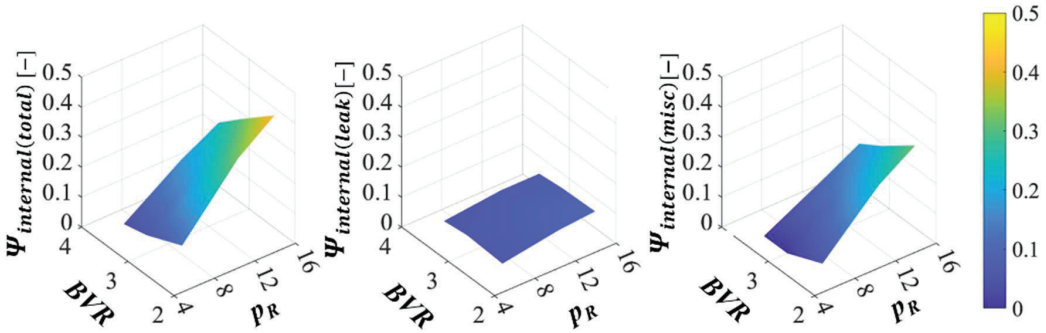

Figure 2. Total (Left), Leakage (middle), Miscellaneous (Right) Internal Losses as a Fraction of Electrical Input Power by Varying p_R and BVR

ratios studied. This is likely because at higher pressure ratios, more cooling oil is injected to maintain the same discharge temperature. As shown by Eqn.(8), the effective leakage area decreases as pressure ratio increases for all BVRs. Illustrating the effect increased oil mass has at clogging leakage paths. $\Psi_{internal(misc)}$ increased for increasing pressure ratio and decreasing BVR. All simulated cases were under compressed for all pressure ratios and BVRs. Meaning the internal compression ratio of the compressor is lower than the system p_R. All under compressed cases require additional input power to overcome unmatched compression. As the p_R increases or BVR decreases, so does the magnitude of the under compression, meaning more input power is required.

Table 1. Simulated Compressor System Losses as a Fraction of Electrical Input Power for Different Pressure Ratios and BVRs [5]

BVR [-]	***2.2***	***2.2***	***2.2***	***3.0***	***3.0***	***3.0***	***3.4***	***3.4***	***3.4***
P_R [-]	***5.7***	***11.3***	***14.9***	***5.9***	***11.5***	***15.3***	***5.9***	***11.5***	***15.3***
Ψ_{ele} [-]	0.04	0.04	0.04	0.04	0.04	0.04	0.04	0.04	0.04
$\Psi_{external}$ [-]	0.26	0.16	0.13	0.28	0.19	0.16	0.28	0.20	0.17
$\Psi_{internal(total)}$ [-]	0.12	0.33	0.42	0.06	0.22	0.31	0.05	0.17	0.24
$\Psi_{internal(leakage)}$ [-]	*0.06*	*0.09*	*0.10*	*0.06*	*0.07*	*0.08*	*0.05*	*0.07*	*0.07*
$\Psi_{internal(misc)}$ [-]	*0.06*	*0.24*	*0.32*	*0.00*	*0.15*	*0.23*	*0.00*	*0.10*	*0.17*
$\Psi_{s\&c}$ [-]	0.11	0.09	0.08	0.12	0.10	0.09	0.12	0.11	0.10
$\eta_{iso,skid}$ [-]	0.46	0.38	0.33	0.51	0.45	0.40	0.51	0.48	0.45

For all simulations, the losses as a fraction of the electrical input power are listed in Table 1. As can be seen, internal losses had the largest effect at increasing electrical input power, varying between 0.05 – 0.42. External losses decrease as a fraction of the electrical input power because the increase in electrical input power outpaced the increase in external losses as p_R increased. All other losses, as a fraction of electrical input power, remained relatively uniform for all cases studied.

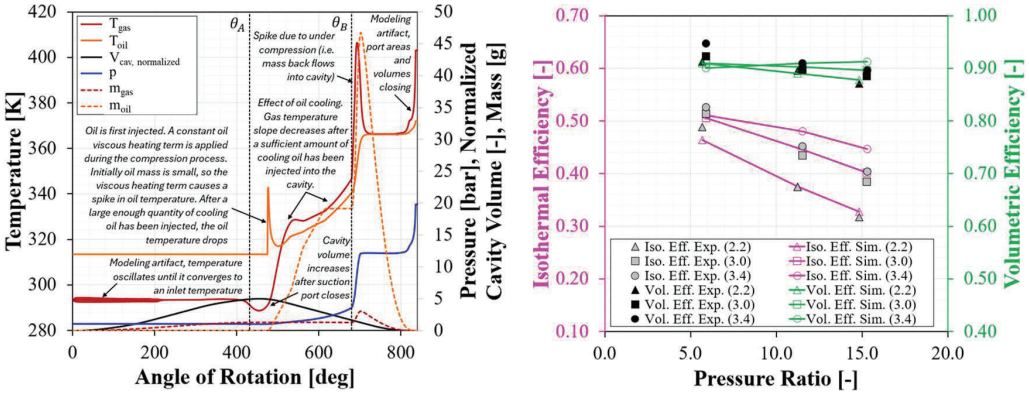

Figure 3. Example of 1D Model Temperature, Pressure, and Mass Outputs (left) and Simulated Versus Experimental Isothermal and Volumetric Efficiency (right)

Skid isothermal efficiency and volumetric efficiency calculated from Eqn.(16) and Eqn.(17), respectively. Figure 3 presents simulated versus most recent experimentally measured skid isothermal and volumetric efficiency [5]. Simulated trends for both efficiencies follow the experimental trend. The maximum absolute relative error between the simulated and

experimentally calculated skid isothermal efficiency is 10.7% and 4.9% for volumetric efficiency. The error is likely because test data was taken during commissioning, not explicitly for characterizing compressor losses. There is some variability in compressor operating parameters, which impacts both isothermal and volumetric efficiency, this primarily effects the BVR 3.4 $p_R = 6$ case.

5. Summary

A 1D model of an oil-injected screw compressor was developed and compared against experimental data from a helium compressor. This model is developed to separate and calculate the losses that occur during the compression process at selected BVR's for various operating conditions. The developed 1D model is applicable for any sized screw compressor assuming the compressor geometry is known and is based on energy and mass balances for a single cavity along the length of the compressor rotor. Compressor test data was utilized to develop an effective leakage area correlation for the compressor simulated in this paper. Simulations were performed to gain a better understanding of how pressure ratio and BVR effect the magnitude of various losses during the helium compression process. Of the internal losses, leakage losses were separated out and accounted for approximately 10% of the electrical input power for all cases studied. This is likely because, at a constant suction pressure, a larger quantity of oil mass is injected at higher pressure ratios to maintain the same discharge temperature, reducing the effective leakage area. Simulated isothermal and volumetric efficiency trends follow experimentally measured trends. In the future all internal and external losses will be separated and independently calculated. Rigorous testing is planned with an experimental compressor skid designed, fabricated and installed at FRIB to refine the 1D model and aid in characterizing compressor losses.

Acknowledgments
This material is based upon work supported by the U.S. Department of Energy, Office of Science, Office of Nuclear Physics and used resources of the Facility for Rare Isotope Beams (FRIB) Operations, which is a DOE Office of Science User Facility under Award Number DE-SC0023633. Travel was funded by the U.S. Department of Energy, Office of Science, Office of High Energy Physics, under Award Number DE-SC0018362.

References

[1] Anthony, S., et al. A One-Dimensional Model of an Oil-Injected Helium Screw Compressor for Cryogenic Refrigeration Systems. in ASME 2024 International Mechanical Engineering Congress and Exposition. 2024.
[2] Abdan, S., Investigation of Mechanical Losses in Oil-flooded, Twin-screw Air Compressors. City, University of London, 2023.
[3] Abdan, S., et al., Oil drag loss in oil-flooded, twin-screw compressors. Proceedings of the Institution of Mechanical Engineers, Part E, 2023. 237(4): p. 1137-1144.
[4] Stosic, N. On Calculation of Leakage Flow in Screw Compressor Elements. in ASME 2020 International Mechanical Engineering Congress and Exposition. 2020.
[5] Knudsen, P., et al., FRIB helium compression system commissioning and performance test results. IOP Conference Series: Materials Science and Engineering, 2020. 755(1): p. 012094.
[6] Tang, Y. Computer aided design of twin screw compressors. 1995.
[7] Stosic, N., et al., Review of Mathematical Models in Performance Calculation of Screw Compressors. International Journal of Fluid Machinery and Systems, 2011. 4.
[8] Budynas, R.G., et al., Shigley's mechanical engineering design. Eleventh edition ed. 2020, New York, NY: McGraw-Hill Education.
[9] Stosic, N., I. Smith, and A. Kovacevic, Screw Compressors: Mathematical Modelling and Performance Calculation. 2005: Springer Berlin Heidelberg.